Journal of Chromatography B, 871 (2008) 261–270

Contents lists available at ScienceDirect

Journal of Chromatography B

journal homepage: www.elsevier.com/locate/chromb

UPLC–TOF-MS for plant metabolomics: A sequential approach for wound marker analysis in *Arabidopsis thaliana*☆

Elia Grata[a,b], Julien Boccard[a,c], Davy Guillarme[a], Gaetan Glauser[a,b], Pierre-Alain Carrupt[c], Edward E. Farmer[d], Jean-Luc Wolfender[b], Serge Rudaz[a,*]

[a] *Laboratory of Pharmaceutical Analytical Chemistry, School of Pharmaceutical Sciences, EPGL, University of Geneva, University of Lausanne, 20 Bd d'Yvoy, CH-1211 Geneva 4, Switzerland*
[b] *Laboratory of Pharmacognosy and Phytochemistry, School of Pharmaceutical Sciences, EPGL, University of Geneva, University of Lausanne, 30 Quai Ernest-Ansermet, CH-1211 Geneva 4, Switzerland*
[c] *LCT-Pharmacochemistry, School of Pharmaceutical Sciences, EPGL, University of Geneva, University of Lausanne, 30 Quai Ernest-Ansermet, CH-1211 Geneva 4, Switzerland*
[d] *Department of Plant Molecular Biology, University of Lausanne, Biophore Building, Quartier Unil-Sorge, CH-1015 Lausanne, Switzerland*

ARTICLE INFO

Article history:
Received 16 January 2008
Accepted 15 April 2008
Available online 20 April 2008

Keywords:
UPLC–TOF-MS
Arabidopsis thaliana
Metabolomics
Signalling
Oxylipins

ABSTRACT

The model plant *Arabidopsis thaliana* was studied for the search of new metabolites involved in wound signalling. Diverse LC approaches were considered in terms of efficiency and analysis time and a 7-min gradient on a UPLC–TOF-MS system with a short column was chosen for metabolite fingerprinting. This screening step was designed to allow the comparison of a high number of samples over a wide range of time points after stress induction in positive and negative ionisation modes. Thanks to data treatment, clear discrimination was obtained, providing lists of potential stress-induced ions. In a second step, the fingerprinting conditions were transferred to longer column, providing a higher peak capacity able to demonstrate the presence of isomers among the highlighted compounds.

1. Introduction

In recent years, much progress has been made in metabolomics to provide a global picture of the molecular organization of multicellular organisms [1]. Many analytical technologies have been enlisted for metabolome profiling [2], mainly based on NMR, GC–MS, direct infusion MS (FIA-MS) or LC–MS. Each of these methods presents advantages and disadvantages in terms of speed, selectivity, sensitivity, dynamic range, robustness and repeatability.

Arabidopsis thaliana is a well-established model plant in biology and different issues related to systems biology have been investigated in this organism. Various NMR-based or MS-based analytical strategies were used. As an example, NMR was found to be successful in identifying metabolite changes in *A. thaliana* that occur after methyl jasmonate treatment [3]. For the detection of wound biomarkers present at very low concentrations, more sensitive detection methods are mandatory and mass spectrometry remains the technique of choice. Direct infusion MS represents a first alternative and, in this respect, direct infusion Fourier transform cyclotron resonance MS (FT-ICR/MS) was found very useful for studies on phenotyping of *A. thaliana* [4]. However, according to the type of crude extracts, direct infusion techniques might suffer from ion suppression problems [5] and a separative step is important to enhance sensitivity and selectivity. Metabolome variations related to stress have been studied with specific GC–MS methods for monitoring the induction of jasmonates and related oxylipins [6], in control and wounded leaves [7] providing an "oxylipin signature" [8]. The major drawback of this approach is its very high specificity, which restricts its use only to the monitoring of volatile and thermally stable oxylipins. Since the expression of various defence genes cannot always be linked to the accumulation of known jasmonates, particularly in leaves distal to the wound site, a more global survey of wound biomarker induction is needed. Non-targeted GC–MS metabolite profiling was selected for the comparative display of gene function in *A. thaliana* [9]. This latter approach however required derivatisation and is not adapted to the analysis of large molecular mass metabolites.

LC–MS represents a powerful alternative, which has been used for profiling a broad range of metabolites in *A. thaliana* [10]. Numerous improvements to decrease analysis time in LC and/or increase

☆ This paper is part of a special volume entitled "Hyphenated Techniques for Global Metabolite Profiling", guest edited by Georgios Theodoridis and Ian D. Wilson.

* Corresponding author. Tel.: +41 22 379 65 72; fax: +41 22 379 68 08.
E-mail address: serge.rudaz@pharm.unige.ch (S. Rudaz).

1570-0232/$ – see front matter © 2008 Elsevier B.V. All rights reserved.
doi:10.1016/j.jchromb.2008.04.021

efficiency and resolution have been proposed. These include usage of monolithic supports [11,12], short columns [13,14] and high temperature LC [15,16]. A confirmed approach to improve chromatographic performance is the use of columns packed with small particles (i.e. sub-2 μm particles). From a theoretical point of view, this particle dimension induces a concomitant increase in efficiency, optimal velocity and mass transfer [17–19]. Therefore, high-throughput separations can be obtained with short column lengths while highly efficient separations are achieved with relatively long columns. Since 2004, manufacturers have introduced a new generation of columns packed with sub-2 μm porous particles [20], which generate reliable performance in comparison with conventional particle size [21,22] but should be used with a dedicated instrumentation such as the UPLC® for ultra performance liquid chromatography [23,24]. Benefits of the UPLC approach have been experimentally highlighted [25–27] and several works recently published using time of flight (TOF) mass spectrometer (i.e. because of the small peak widths afforded by the UPLC and the necessity to have a high acquisition rate) [28–30]. An interesting paper demonstrated that a differentiation between red and white Ginseng qualities could be obtained [31] but to our knowledge, UPLC–TOF-MS in plant metabolomics has only been scarcely reported.

In our previous work, a two-step LC–TOF-MS strategy was developed for the detection and localisation of stress-induced metabolites in *A. thaliana*. The approach was based on the analysis of total TOF-MS spectra of numerous plant specimens (metabolite fingerprinting) followed by high-resolution UPLC separation of selected sample pools for biomarker deconvolution (metabolite profiling) [32]. In the present study, the two-step strategy was revised to optimise the use of UPLC–TOF-MS for both high-throughput 'metabolite fingerprinting' and confirmatory 'metabolite profiling' analyses. This was achieved according to both fundamental chromatography considerations and reasonable criteria for plant metabolomics regarding sensitivity, resolution and throughput capacity. The 'metabolite fingerprinting' experimental conditions were selected for fast separations using short UPLC columns which ensured satisfactory LC resolution. The data were treated by taking the advantage of both chromatographic information and accurate mass determination. The confirmatory analysis conditions were obtained by a geometrical gradient transfer to provide a precise separation and localisation of the biomarkers of interest with a high peak capacity analysis. In this respect, the study of minor but significant metabolome variation related to wounding at different time points in *A. thaliana* was investigated for a relatively high number of plant specimens. The study was extended to the analysis of leaves distal to the wound site.

2. Experimental

2.1. Solvents

The solvents used for the extractions were methanol (MeOH) from VWR (Leuven, Belgium) and isopropanol (IPA) from SDS (Peypin, France). Acetonitrile (ACN) and water were of LC–MS grade from Fisher Scientific (Loughborough, UK). The formic acid of LC–MS grade, used as eluent additive, was obtained from Sigma–Aldrich (Steinheim, Germany).

2.2. Plant growth, wounding treatment

A. thaliana (Ecotype Columbia-0) were grown for 7 weeks (developmental growth stage 3.70 according to Boyes et al. [33]) at 22 °C, 70% relative humidity, and with 9 h light at 100 μmol m^{-2} s^{-1} per day. Half of the rosette leaves of *A. thaliana* plants were crushed across the apical lamina with forceps (30–40% of the leaf area) representing the local situation. The unwounded half of the rosette represents the distal situation. Plants were incubated in the light for 90 min, 3, 6 and 24 h after which the leaves were harvested and immediately frozen in liquid nitrogen. Control plants were harvested at the beginning of the experiments. Samples were placed in a −80 °C freezer until extraction [32].

2.3. Extraction procedure

Approximately 500 mg of leaf tissues were ground and extracted with 5 mL IPA using a ball mill (ball diameter 2 cm, frequency 30 Hz, and time 2 min) (Retsch MM200, Schieritz & Hauenstein AG, Arlesheim, Switzerland). The extracts were dried under a stream of nitrogen. The IPA extracts were purified by simple sample preparation (SPE) (Waters Sep-Pak C18, Vac 1 cm^3, 100 mg). After cartridge conditioning (1 mL MeOH, 1 mL MeOH–H_2O (85:15, v/v%)), 5 mg of extract was diluted in 500 μL of MeOH–H_2O (85:15, v/v%), loaded and washed with 1 mL MeOH–H_2O (85:15, v/v%) to remove chlorophyll and other lipophilic pigments. The residue was finally dissolved in 200 μL of MeOH–H_2O (85:15, v/v%) [32].

2.4. LC–MS analyses

LC–MS analyses were performed on a Micromass-LCT Premier Time of Flight (TOF) mass spectrometer (Waters, MA, USA) with an electrospray interface and coupled with an Acquity UPLC system (Waters, MA, USA). ESI conditions: capillary voltage 2800 V, cone voltage 40 V, MCP detector voltage 2650 V, source temperature 120 °C, desolvation temperature 250 °C, cone gas flow 10 L/h, desolvation gas flow of 550 L/h. Detection was performed in positive and negative ion modes in the m/z range 100–1000 with a scan time of 0.25 s for the rapid gradient and 0.5 s for the long gradients in centroid mode. For the dynamic range enhancement (DRE) lockmass, a solution of leucine–enkephalin (Sigma–Aldrich, Steinheim, Germany) at 5 μg/mL was infused through the Lock Spray™ probe at a flow rate of 20 μL/min with the help of a second LC pump (Shimadzu LC-10ADvp, Duisburg, Germany).

The separations were carried out on Waters Acquity UPLC columns at 35 °C (BEH C18: 1.0 mm × 50 mm and 2.1 mm × 150 mm, 1.7 μm) with the following solvent system: A = 0.1 vol.% formic acid–water, B = 0.1 vol.% formic acid–ACN. For the 1.0 mm × 50 mm column, the gradient elution was performed at a flow rate of 300 μL/min using: 5% B for 0.3 min, 5–98% B in 6.7 min and holding at 98% B for 3 min.

For the 2.1 mm × 150 mm column, the gradient elution was performed at a flow rate of 300 μL/min using: 5% B for 8.9 min, 5–98% B in 92.8 min and holding at 98% B for 18 min. Finally for the two 2.1 mm × 150 mm columns coupled in series, the gradient was performed at a flow rate of 200 μL/min using: 5% B for 27.2 min, 5–98% B in 278.6 min and holding at 98% B for 20 min.

2.5. Kinetic plots

In order to compare different LC analytical techniques, it is mandatory to simultaneously consider the mobile phase flow rate, chromatographic efficiency and generated backpressure. Furthermore, each of these parameters may depend on instrumental limitations and column geometry. While Van Deemter or Knox plots are easy to interpret, the information given by $H = f(u)$ curves is partial because the permeability of the support is not taken into account. As an alternative representation, kinetic plots $N = f(t_0)$ have been introduced by Giddings [17] to compare the limits of LC and GC in terms of analysis time and efficiency. In 1997, Poppe [19] used kinetic plots to compare different LC and capillary elec-

trochromatography (CEC) approaches. Up to now, these curves were not extensively applied, due to the complexity of the construction methodology (based on a numerical iteration procedure [19]). Recently, Desmet et al. [22,34] proposed a simplified approach based on experimental Knox data (u, H) and permeability values (K_{v0}). For this purpose, only two equations are necessary to transform experimental data into extrapolated plots of analysis time versus efficiency:

$$N = \frac{\Delta P_{max}}{\eta}\left(\frac{K_{v0}}{u_0 H}\right)_{experimental} \quad (1)$$

$$t_0 = \frac{\Delta P_{max}}{\eta}\left(\frac{K_{v0}}{u_0^2}\right)_{experimental} \quad (2)$$

where N is the efficiency, t_0, the column dead time, u_0, the mobile phase velocity and H, the plate height. In both equations, a scaling value for the pressure drop ΔP and the mobile phase viscosity η is used.

2.6. Data treatment

Data preprocessing was performed with MarkerLynx™ software (Waters, MA, USA) and MATLAB® 7 (The MathWorks, USA). ANOVA filtering, multivariate analysis by PCA and HCA were performed with MATLAB® 7 (The MathWorks, USA). Partial least squares discriminant analysis (PLS-DA) was performed with the PLS Toolbox (Eigenvectors Research Inc., USA). Orthogonal signal correction (OSC) filter was calculated with SIMCA-P© (Umetrics, Sweden). Leave-one-out procedure was applied for models' cross-validation.

3. Results and discussion

Beside the issues related to the determination of key markers, metabolomic studies have revealed the difficulties that arise when trying to highlight *de novo*-induced compounds due to both their very restricted amounts and the convoluted nature of the biological extracts. Therefore, the identification of minor-induced compounds versus constitutive metabolites remains a very challenging analytical problem. In our previous work related to the search for wound biomarkers in *A. thaliana* [32], a two-step strategy was developed as a result from a compromise that needs to be made between throughput and performance. Briefly, it consisted of a metabolite fingerprinting of a large number of samples followed by a metabolite profiling of specific selected pools, characteristic for a given physiological state. Crude leaf IPA extracts were first analysed with a ballistic gradient on a conventional LC support hyphenated to TOF-MS within a short analytical time period to avoid instrument variations, to rapidly obtain information on samples that exhibit significant differences and evaluate the sample-to-sample variability. Due to the short column length, the gradient profile and the nature of the injection solvent, the retention time (t_r) information was discarded and the MS information treated as total mass spectra (TMS). To decrease the individual variability, a careful pooling of individual samples was based on a multivariate data analysis [35]. The precise localisation and the accurate mass confirmation of putative stress biomarkers were achieved for several compounds of interest. To improve the efficiency of detection of representative minor biomarkers in metabolite fingerprint for *A. thaliana*, the introduction of a UPLC–TOF-MS screening step was investigated.

3.1. Criteria for plant metabolomics

Based on our previous experiments, different criteria were retained to optimise the detection of minor key biomarkers. Due to the complexity of the samples, a relatively elevated average retention factor in gradient analysis (k_e = 10) was selected to obtain sufficient chromatographic resolution. Particular attention was paid to improve performance in the initial screening determination to enable use of both retention and MS information, improving the data treatment compared to TMS. This was achieved using a chromatographic gradient, which resulted in decreased noise and minimised ion suppression effects. For metabolite fingerprinting, analysis time was maintained as short as possible (lower than 10 min for a complex plant extract) and efficiency values kept in a moderate range (5000–15,000 plates). For metabolite profiling, efficiency had to be increased to much higher values (30,000–70,000 plates), while maintaining acceptable analysis time (lower than 3 h).

3.2. Criteria for chromatography

In order to achieve the criteria set for plant metabolomics, the kinetic plots corresponding to different LC approaches were found to be very useful. This representation (i.e. t_0/N^2 as a function of N) has been evaluated for columns packed with 5 and sub-2 μm particles, UPLC and monolithic supports (Fig. 1). The kinetic plots were calculated with the help of a free Excel spreadsheet from the group of Desmet et al. [36], for these four different analytical approaches to anticipate the optimal set-up for the metabolomic platform. H and ΔP values, experimentally obtained for several linear velocities ranging from 0.13 to 8.26 mm/s, have been transformed into $N = f(t_0/N^2)$ curves. Mobile phase viscosity was set to a constant value of 0.85 cP (corresponding to a mixture of 40:60 ACN:water at ambient temperature). In this representation, each type of data point represents a column that differs in length, which gives the maximal system pressure drop. The latter was fixed at 1000 bar for UPLC system, 400 bar for columns packed with 5 and sub-2 μm particles and 200 bar for monolithic supports, according to the manufacturer specifications (Merck, Darmstadt, Germany). The best chromatographic performance expressed as efficiency for a given analysis time, or analysis time for a given efficiency corresponds to the lowest curve. The maximal achievable efficiency within a given set of conditions corresponds to the vertical asymptote, observed on the left side of each curve.

Two zones have been distinguished in Fig. 1, the first one exhibits medium–low values of efficiency (<15,000) while the second presents a higher number of theoretical plates (>30,000). For an efficiency value in the range (5000–15,000), sufficient for the fingerprinting experiments, the best performance is always reached with the sub-2 μm diameter particles support. In this range, columns packed with 5 μm particles represent the worst approach considering analysis time for a given efficiency, while monolithic and sub-2 μm particles packings present some obvious advantages in terms of column dimension. It is also important to note that the difference between sub-2 μm used at 400 or 1000 bar (UPLC) was not pronounced. To obtain high-throughput separations, the reduction of particle size is essential while the increase in maximal system pressure to a value higher than 600 bar is not an absolute criterion as demonstrated elsewhere [21].

The second zone seen in Fig. 1 represents efficiency values in the range (30,000–70,000), which corresponds to high-resolution requirement compatible with confirmatory analyses. The use of sub-2 μm particles at a conventional pressure (400 bar) leads to a maximal achievable efficiency of about 40,000 plates. The lowest analysis time for a given efficiency is achieved with monoliths (t_0 = 100 s for 30,000 plates) and UPLC (for example, t_0 = 100 s for 45,000 plates). Monolithic supports are particularly interesting for values higher than 90,000 (see arrow 3) and were already selected

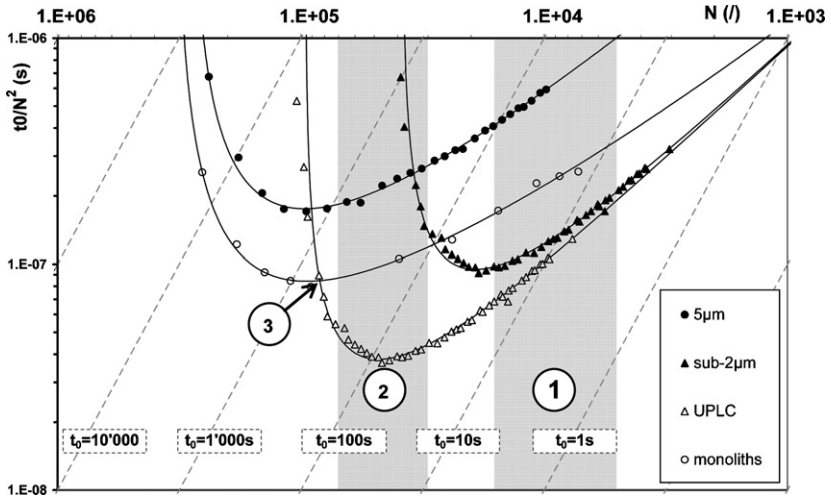

Fig. 1. Comparison of several approaches to obtain high-throughput and high-resolution separations, using kinetic plot representations ($t_0/N^2 = f(N)$) for butylparaben. (●): Conventional LC, XTerra RP_{18} 4.6 mm × 150 mm, 5 μm with ΔP_{max} = 400 bar, (○): monolithic support, Chromolith C_{18} 4.6 mm × 100 mm with ΔP_{max} = 200 bar, (▲): sub-2 μm, Hypersil GOLD C_{18} 2.1 mm × 50 mm, 1.9 μm with ΔP_{max} = 400 bar, (△): UPLC, Acquity Shield C_{18} 2.1 mm × 50 mm, 1.7 μm with ΔP_{max} = 1000 bar. For all tested approaches, η = 0.85 cP, Dm = 1.10^{-9} m^2/s.

in some metabolomic studies [37–39]. Since chromatographic efficiency is directly related to maximal backpressure (according to Eq. (1)), an increase from 400 to 1000 bar (UPLC) allows a gain in efficiency by a factor 2.5. Therefore, for the efficiency range (30,000–70,000), the use of UPLC gives the most powerful performance. Hence, the use of sub-2 μm particles stationary phase at 1000 bar appeared to be the best strategy for both high-throughput and high-resolution profiling of crude plant extracts. Furthermore, since the same stationary phase chemistry could be maintained during the whole process, it allows the precise comparison of the obtained profiles with a careful gradient transfer procedure [40].

Finally, to obtain the maximum efficiency with respect to constraints on analysis time and generated backpressure, column length and mobile phase flow rate were also adapted with the help of kinetic plots (data not shown). For columns packed with sub-2 μm particles with a maximal pressure of 1000 bar, 70,000, 35,000 and 7500 plates could be obtained with column length of 300, 150 and 50 mm, respectively. According to the required efficiency, the mobile phase flow rates for 2.1 mm ID columns were estimated. To reach efficiency in the range of 30,000–70,000 plates, the flow rate should be equal to 250 μL/min with the 300 mm column length. To generate about 7500 plates with the 50 mm column length, the flow rate must be set to 1300 μL/min. Since the latter was incompatible with ESI-MS without splitting, a 1 mm ID column was selected with an identical mobile phase linear velocity, corresponding to a 300 μL/min flow rate.

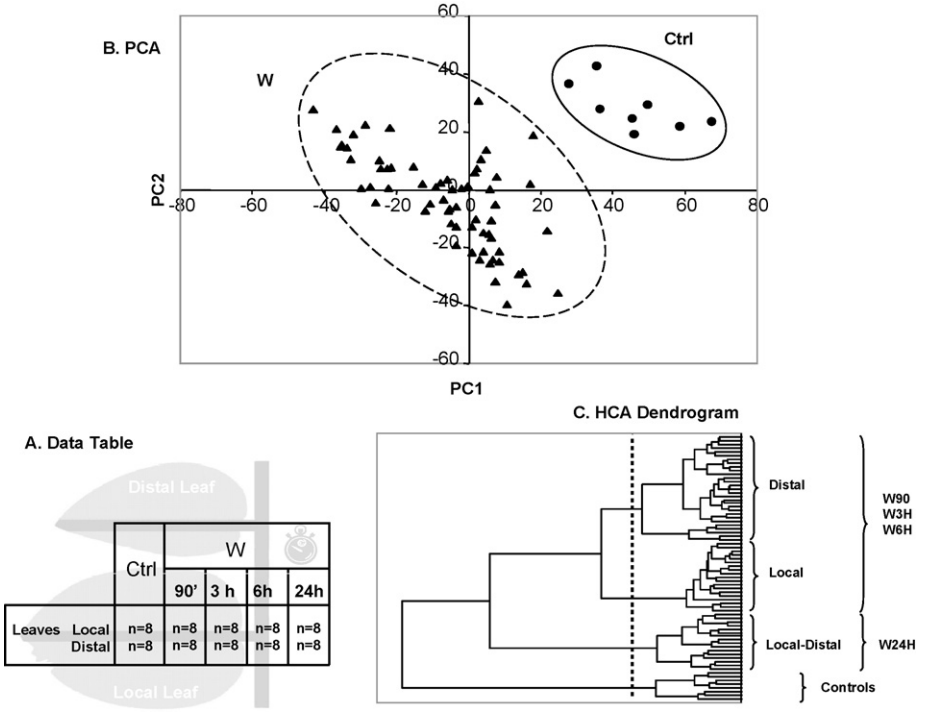

Fig. 2. (A) Table of experiments. (B) PCA score plot (PC1 15% vs. PC2 10%). (C) HCA dendrogram (Euclidean distances and Ward aggregation method). Control plants (Ctrl) symbolized by circles and wounded plants (W) by triangles.

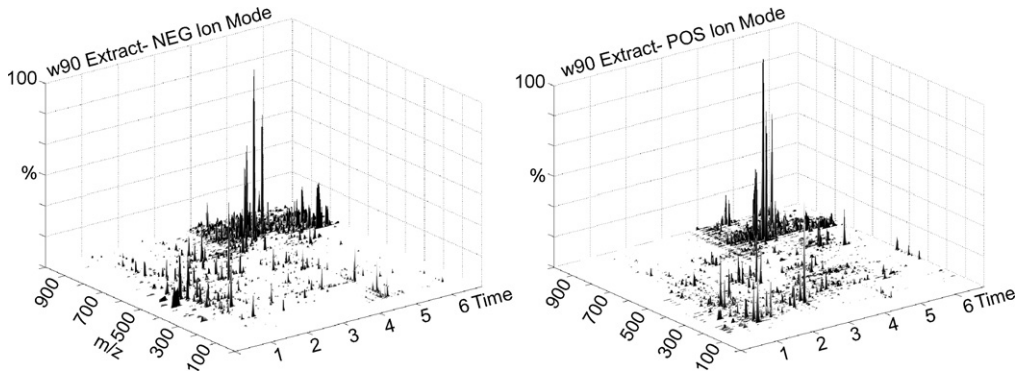

Fig. 3. Metabolite fingerprinting. 3D ion maps obtained in negative (NEG) and positive (POS) ionisation mode for wounded plant specimens harvested after 90 min (W90).

3.3. High-throughput metabolite profiling of A. thaliana

As previously observed [32], different induced compounds were evidenced in local leaves by wounding with forceps. For a better understanding of the complex phenomena that govern plant response, a more comprehensive study of the chemically mediated events that trigger response to stress is however needed, particularly with respect to long distance signalling. Several studies demonstrated that one or more members of the jasmonate family can be translocated over long distances to regulate the systemic response to wounding [41]. As an example, Li et al. have shown that (pro)systemin is required for the production of a long distance signal whose recognition in distal leaves depends on jasmonate signalling in tomato plants [42]. Experiments on a mutant with a loss of function of an acyl-CoA oxidase (ACX1A) catalyzing the first step of jasmonic acid (JA) biosynthesis indicated the absence of the systemic wound signal [43].

In the case of *A. thaliana*, the situation regarding the accumulation of wound markers in different parts of the plant should be clarified. To provide more clues on both local and systemic response

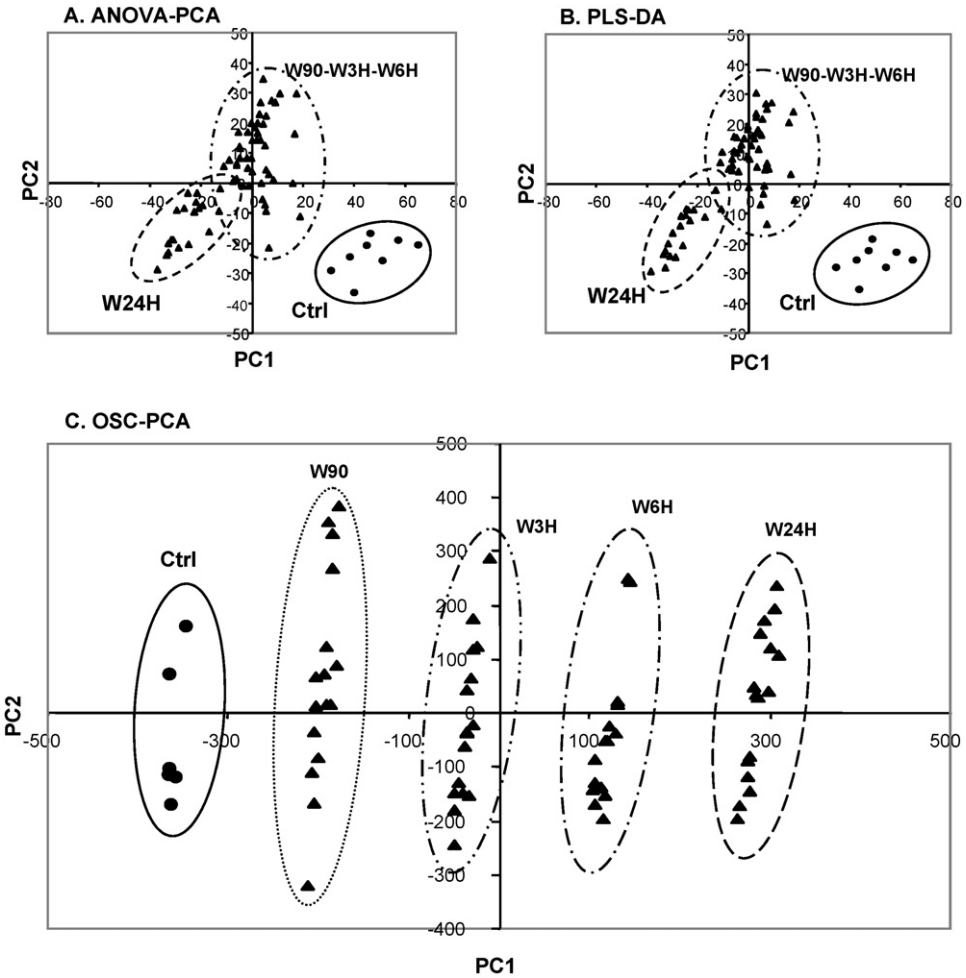

Fig. 4. ANOVA-PCA (PC1 22% vs. PC2 14%), PLS-DA (LV1 17% vs. LV2 10%) and OSC-PCA (PC1 15% vs. PC2 10%) score plots. Control plants (Ctrl) symbolized by circles and wounded plants (W) by triangles.

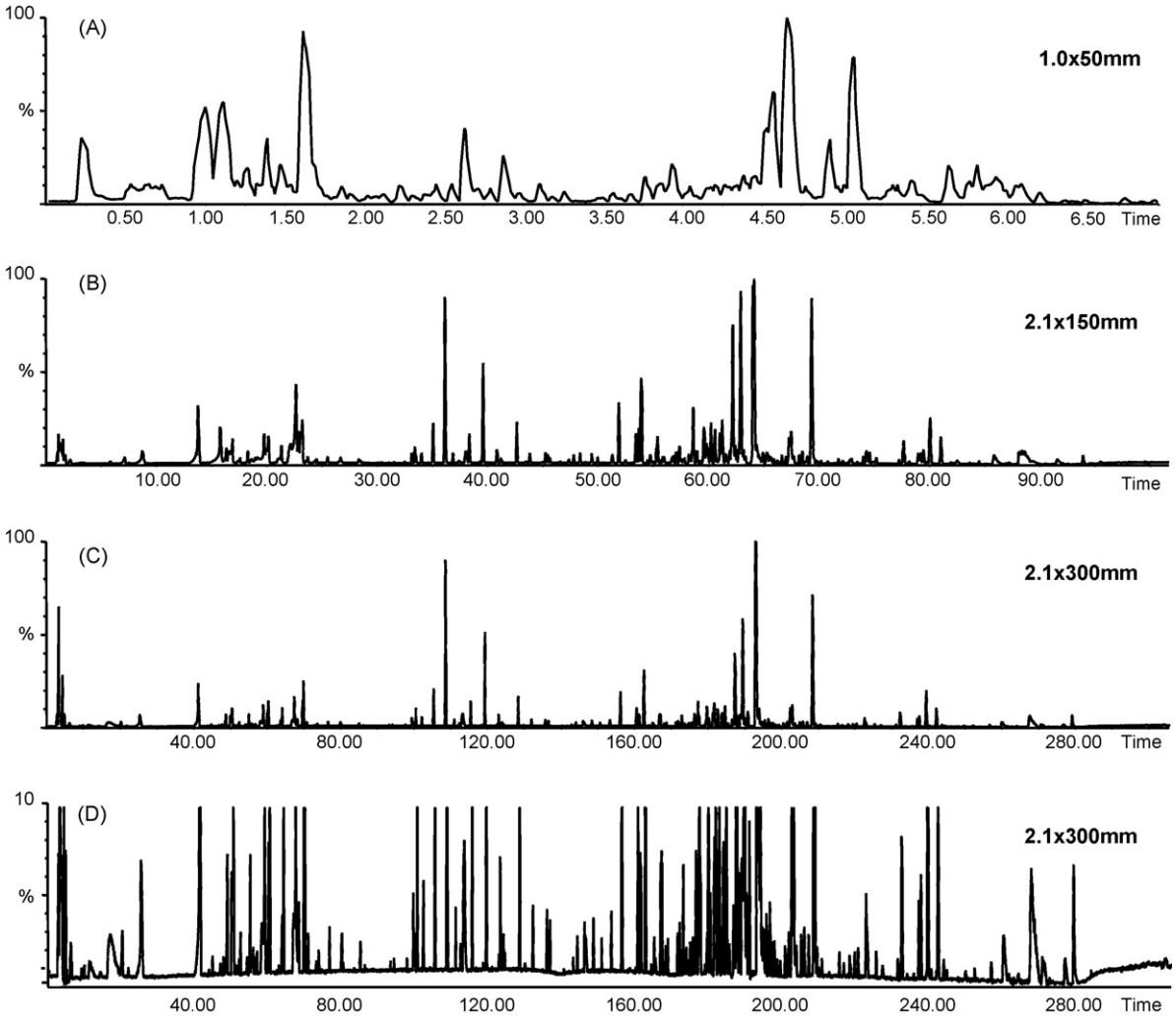

Fig. 5. Example of geometrical gradient transfer. Chromatograms obtained by UPLC–TOF-MS in negative ionisation mode of a wounded pooled extract (A) on a 1.0 mm × 50 mm, (B) on a 2.1 mm × 150 mm and (C) on a 2.1 mm × 300 mm column. (D) Zoom on the 10% of intensity for the BPI obtained on a 2.1 mm × 300 mm column.

to wounding, our investigations utilised several time points and different tissue locations (wounded and distal leaves). For this purpose, plants were wounded and harvested at different times (90 min, 3, 6, and 24 h), based on the study performed by Reymond et al. [44]. Indeed, the maximal accumulation of JA in this system has been reported to occur 90 min after wounding, however monitoring up to 24 h was important to identify the substances responsible for the late response (see Fig. 2A). For the spatial situations, the local wounded leaves and the distal leaves representing the opposite unwounded part were studied. Each situation was characterised in eight independent plant specimens. A control with the same number of samples was included in the study. A total of 80 plants were grown, wounded, harvested and prepared to be independently analysed with the proposed screening approach using positive and negative ESI mode.

A SPE was included prior to UPLC analysis. This step was optimised to obtain a maximum number of metabolites and to prevent any instrumental contamination and column clogging by lipophilic pigments. To achieve the best compromise between sensitivity and extra-column band broadening effects, the injected quantity was fixed at 5 μL MeOH–H_2O (85:15, v/v%). This sample pre-treatment was evaluated by analysis of control and wounded leaf extracts after the SPE. An efficient removal of the most lipophilic compounds was provided and blank injection between runs demonstrated the absence of carry over effects. Based on the above-mentioned considerations, a UPLC gradient separation was optimised on a short column length (1.0 mm × 50 mm) with the maximum available flow rate (300 μL/min, 790 bar). Gradient slope was thus calculated to obtain an analysis time of less than 7 min with a $k_e = 10$. Initial and final compositions were selected to provide maximal information in one linear gradient (5–98% MeCN). In Fig. 3 an example of UPLC–TOF-MS data set is displayed which demonstrated the complexity of the analysed extract and that both positive and negative ionisation modes are complementary in the metabolite fingerprinting step.

It has to be noted that the selected column diameter (1 mm ID) allows decreasing the minimal sample amount required for metabolite fingerprinting which could be reduced to 50 mg of fresh leaves (ca. 1/10 of a 7-week rosette). The TOF system was operated in ESI and analyses acquired using the Lock Spray™ interface to ensure mass accuracy. Thanks to the TOF-MS, extraction of ions with a precision of <5 ppm was possible for an efficient discrimination of sample constituents. Furthermore in terms of sensitivity no compromise related to duty cycle was needed while fast scanning and extend mass range (m/z 100–1000) was achieved for a good LC-peak resolution. This fast gradient was repeated on more

than 300 independent sample injections without noticeable loss of chromatographic performance or changes in both retention time and mass accuracy.

3.4. Data treatment of the rapid UPLC–TOF-MS

Because hyphenation of UPLC separation and MS detection produces large three-dimensional information (retention time × m/z × intensity) (Fig. 3) and due to the high number of samples analysed, preprocessing of the data was required.

In a first step, noise filtering, peak detection and matching were concomitantly performed, making use of both UPLC high peak capacity and resolving chromatographic power and the high mass accuracy of TOF-MS detection. The method parameters were: retention time range, 0.3–6.8 min; tolerance, 0.5 min; mass range, 100–1000 Da; mass tolerance, 0.05 Da. Noise elimination level was set to 25.00 and isotopic peaks excluded from the analysis. No internal standard for peak retention time alignment was needed and no mass exclusion list was defined. The selected retention time range discarded the injection time area where co-elution of polar constituents probably occurred. Collection parameters included a mass window of 0.05 Da without minimum intensity. The UPLC method retention time repeatability was initially checked and peak retention time constancy confirmed (RSD lower than 0.5%). After completing the integration parameters, a report of peaks based on areas was generated for each sample and a comprehensive list of the detected components created. For this purpose, corresponding peaks were used to build a data table. Signals of different samples were considered to be similar when they simultaneously fulfilled both retention time (0.5 min tolerance) and m/z value (0.05 Da tolerance) criteria. Each detected peak was normalized against the sum of all signals within the sample (TIC normalization). When a peak was not detected in a sample, the related value was set to zero. Positive and negative ion data were independently preprocessed before merging. The final data table consisted of retention time and positive or negative m/z data pairs as labels, which was exported to perform multivariate analysis. The latter was used to produce interpretable projections of samples in a reduced dimensionality (score plots) and highlight putative biomarkers responsible for the group separation (loading plots). Statistical methods proposed by the MS acquisition software such as principal components analysis (PCA) were initially used. However, the dataset was also investigated with several complementary analysis tools.

In a first approach PCA provided an unsupervised data reduction without using class information. Samples were compared to assess metabolites level modifications occurring either in local leaves at different times after wounding and in leaves in distal position to the wound site. Different scaling methods (Unit Variance and Pareto) were performed. Because no relevant differences on our data set were observed, results presented in this paper were achieved with UV-scaling.

As presented in Fig. 2B, controls were clearly distinguished from wounded leaves on the PCA scatter plot (PC1 vs. PC2), but further information considering clusters formation could hardly be deduced. Therefore, hierarchical cluster analysis (HCA) was performed to clarify the class partition, based on the samples projections on the principal axes and 95% of the original variance was used by selecting 58 PCs and HCA was obtained using the Ward aggregation method (Euclidean distances) [35].

On a spatial consideration, the HCA dendrogram showed control samples clearly separated from local and distal wounded leaves. Furthermore, it has to be noticed that local and distal leaves presented distinct patterns considering early wounding times (i.e. 90 min, 3, and 6 h), while local and distal samples showed convergent metabolite profiles 24 h after wounding. In addition, distal leaves were much more similar to locally wounded leaves than to controls. These results strongly suggest the rapid induction of low mass regulators after plant wounding. Fig. 2C shows HCA dendrogram of the clusterisation obtained in both temporal and spatial dimensions.

PCA loadings were then investigated. Because of the large number of peaks detected (>3000 variables), leading to difficultly exploitable complex plots, the most significant ions were examined in more detail using a contribution table that ranked the ion's contributions to the projection axes (data not shown). This ranking

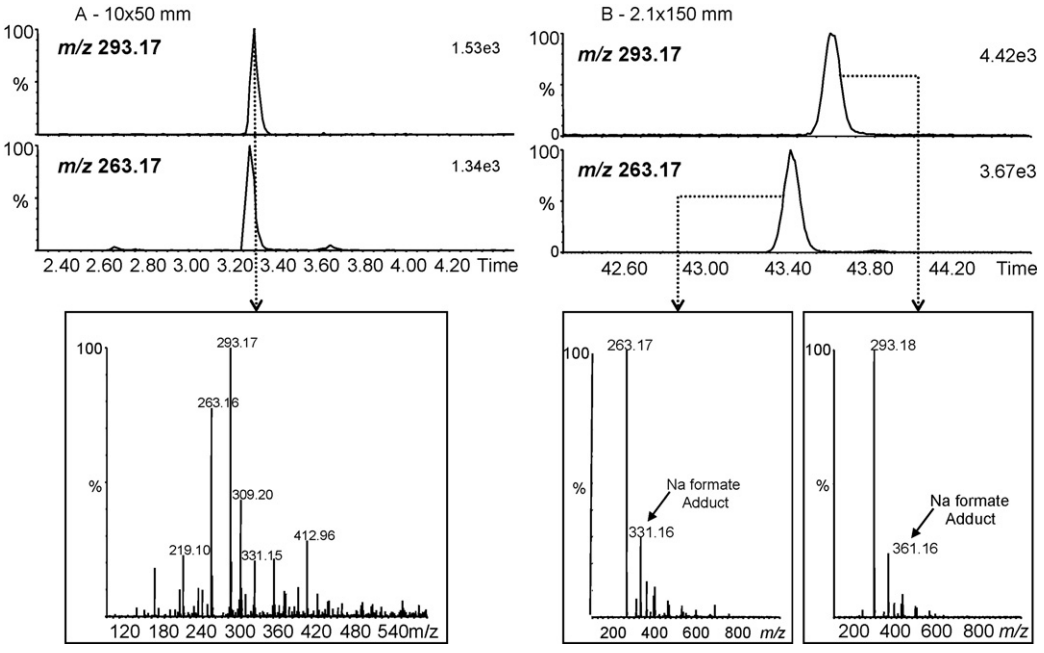

Fig. 6. (A) Traces for extracted ions m/z 293.17 and 263.17 in metabolite fingerprinting and MS spectrum at 3.30 min. (B) Traces for extracted ions m/z 293.17 and 263.17 in the metabolite profiling and MS spectrum at peak apex.

list, based on PCA loadings, suggested many high molecular weight wound markers responsible for metabolite fingerprint differences. However, low mass regulators such as oxylipins, well known stress-induced metabolites, were poorly represented.

In order to highlight differences between groups of plants, a filter procedure was applied to emphasize information linked to group separation. Multiple univariate ANOVA was performed prior to PCA as described in Ref. [35] without amplifying the separation between groups of samples and significantly reducing the number of potential metabolites (see Fig. 4A). Classification models were then evaluated and PLS-DA performed to find a model describing maximum partition between pre-defined classes. PLS-DA consists in a classical PLS regression where the response variable contains categorical dummy values describing the categories. In practice, a value of zero indicates that a sample is not in the modeled class and a value of one indicates a sample in the modeled class. PLS-DA components are built by trying to describe the set of explanatory variables and predict the groups concomitantly. As HCA, the PLS-DA score plot showed three main clusters (Fig. 4B) but brought no additional information considering the ranking table of contributions. In situations where a PLS model captures a very large amount of predictor block (X) variance in the first factor but gets very little of the predicted variable (Y), it can be helpful to remove extraneous variance from X that is unrelated to Y. This can be achieved using OSC, a multivariate filtering procedure which emphasizes discriminant information and down-weight common patterns by finding directions in X that describe large amounts of variance orthogonal to Y. OSC with two components filtering 15.2% of the initial information was used. A different time series partition of samples was obtained using OSC-PCA and allowed to distinguish every sample group along the first axis as presented in Fig. 4C. The investigation of the contribution list to the time clusters formation in the various representations pointed out some differences according to the data analysis. In ANOVA-PCA and PLS-DA, the first axis highlighted either continuously increasing or decreasing metabolite profiles with a plateau between 90 min and 6 h while in OSC-PCA, the most contributive compounds highlighted a linear concentration modification. Thus, the shape of the most contributing kinetic profiles being directly related to the statistical treatments, a comprehensive approach involving different multivariate methods leading to complementary information was required and will be exploited on a more phytochemical perspective elsewhere. Finally, pair-wise comparisons between control and wounded sample groups were exploited in OSC-PCA to generate specific ranking lists. Consequently, each wounded plant group was separately analysed with control leaf samples to identify stress-induced ions corresponding to a given time (90 min, 3, 6, and 24 h). For instance, 4 out of the 10 first compounds acting for the differentiation between control and 90 min wounded leaves were highlighted as probable known metabolites.

3.5. Transfer of the high-throughput gradient to highly efficient metabolite profiling

An unambiguous molecular weight identification from possible fragments or adducts was difficult to ascertain in metabolite fingerprinting and clean spectra were needed. An accurate method

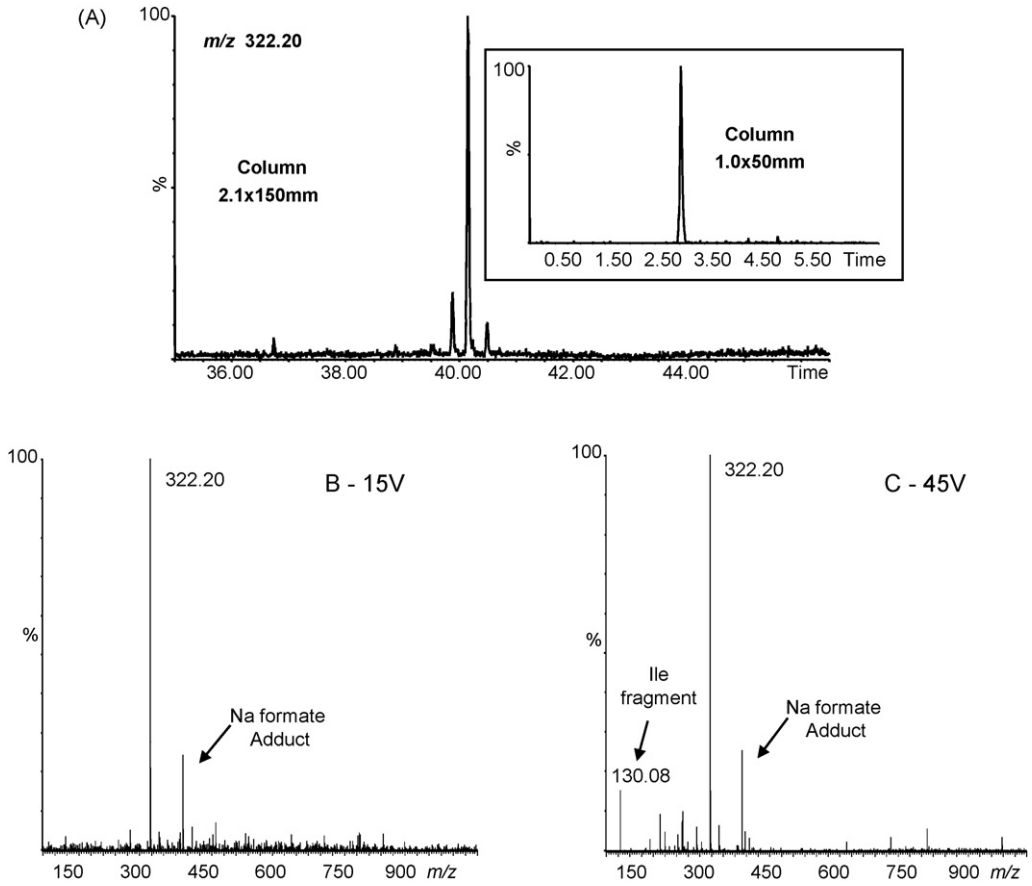

Fig. 7. (A) Separation of m/z 322.20 isomers obtained on a 2.1 mm × 150 mm column. In the inset the m/z 322.20 trace on a 1.0 mm × 50 mm column is shown. (B) Mass spectrum obtained for the m/z 322.20 ion without CID (aperture 1: 15 V). (C) Mass spectrum obtained for the m/z 322.20 ion with upfront CID (aperture 1: 45 V).

transfer between the metabolite fingerprinting and the metabolite profiling was thus mandatory for the precise localisation of the potential biomarkers determined by data treatment. This high-resolution analysis was important to avoid co-elution problems related to the convoluted nature of the extract and to determine the molecular mass of the wound-induced compounds. The metabolite profiling step gave the separation of regio- or diastereo-isomers and exploitable pseudo MS/MS spectra by in-source collision-induced dissociation (CID).

While the screening method provided about 7000 theoretical plates (see Fig. 5A), two solutions were investigated to obtain highly efficient separation for confirmatory analyses: (1) one single 150 mm column generating about 35,000 plates at a flow rate of 300 μL/min and (2) two 150 mm columns coupled in series providing 70,000 plates at a lower flow rate (200 μL/min). Because the same stationary phase chemistry was available, a strict geometrical transfer, avoiding changes in selectivity was performed using the basic rules for method transfer [40,45,46]. Gradient profile conditions were obtained taking into account the change in column geometry using a freely usable Excel available on internal website [47].

As presented in Fig. 5B, the separation obtained with the 2.1 mm × 150 mm column generated superior peak capacity over the 1.0 mm × 50 mm (see Fig. 5A) while selectivity between both separations was maintained, with apparent retention factor differences always lower than 1%. The separation on the coupled support (300 mm column length) (see Fig. 5C) generated, as expected, twofold higher efficiency. Compared to the original separation, a small shift in apparent retention was observed (about 4%). Fig. 5D represents a zoom at 10% of the total intensity, where most of the wound biomarkers are detected, and highlights the plant matrix complexity. Concerning the analysis time, it was increased by a factor 14 and 44 for the 150 and 300 mm column lengths, respectively. This was not a critical issue because confirmatory experiments were only performed on pooled samples.

As indicated above, high peak capacity separation was required for the localisation of different selected compounds, highlighted by the data treatment. As an example, the fingerprinting data treatment revealed a clear induction of the ion *m*/*z* 263 in the wounded leaves. Because this ion was coeluting with other major peaks (e.g. *m*/*z* 293), it did not represent the base peak of the MS spectra (see Fig. 6A). It was thus difficult to attribute *m*/*z* 263 to a deprotonated molecule or a fragment. The high-resolution profile of the wounded and control pools confirmed the wound induction *m*/*z* 263 and its absence in the controls. Thanks to the extended column length, *m*/*z* 263 was separated from the interfering compound, *m*/*z* 293, a constitutive metabolite not altered by the effect of wounding (see Fig. 6B). A clean MS spectrum was obtained for *m*/*z* 263 with the deprotonated molecule and the presence of sodium formate adducts. With the high mass accuracy of TOF-MS, this compound was associated to the molecular formula $C_{16}H_{23}O_3$ (*m*/*z* 263.1637, calc. mass 263.1647, error 3.8 ppm), corresponding to an oxidised C16 fatty acid [32]. This oxylipin, known as dinor-oxo-phytodienoic acid (dnODPA), has been previously observed by targeted GC–MS profiling methods [48] and further confirmed by comparative analysis on an available standard (data not shown).

Isomer identification was achieved with the compound *m*/*z* 322. While only one peak was detected in the fingerprinting step, a baseline separation of three isomers was obtained for this compound in the confirmatory analysis (see Fig. 7A). These isomers were identified based on their identical accurate mass (*m*/*z* 322.2028, $C_{18}H_{28}NO_4$, calc. mass 322.2018, error 3.1 ppm, Fig. 7B) in normal TOF conditions (aperture 1: 15 V). Structural information was further obtained by analysing the extract by in-source CID (aperture 1: 45 V). As presented in Fig. 7C, a fragment ion at *m*/*z* 130 (*m*/*z* 130.0874, $C_6H_{12}NO_2$ calc. mass 130.0868, error 4.6 ppm) was recorded. The associated neutral loss (192.1150, $C_{12}H_{16}O_2$) matched with the mass of dehydrated JA. The *m*/*z* 322.202 was determined to be a conjugate of JA and the detected fragment ion at *m*/*z* 130 corresponded to the amino acid leucine (Leu) or isoleucine (Ile). JA-Ile is a biologically active form of JA [49]. The presence of isomers might be related to an epimerisation at C-7, leading to a *cis–trans* isomerisation of the cyclopentanone ring. Further isomerisation of the double bond is also possible. These changes cannot be assessed based on upfront CID-MS experiments. Other members of the jasmonate family were efficiently detected based on the same strategy. Other compounds highlighted by this approach were isolated after up-scaling of the metabolite profiling UPLC conditions to semi-preparative HPLC for further characterisation by microflow NMR technique at the microgram scale and are discussed elsewhere [50].

4. Conclusion

UPLC–TOF-MS represents a powerful analytical platform for the sensitive detection of stress biomarkers. The evaluation of sub-2 μm column based on fundamental chromatography aspects has demonstrated that this technology represents an attractive approach to achieve both metabolite fingerprinting and profiling analyses in plant metabolomics.

Metabolite fingerprinting applied to numerous leaf samples has yielded high quality LC–MS data, thanks to high sensitivity of detection and low retention times variability. Various data treatments gave several informative lists of potential wound biomarkers and achieved adequate pool formation with selected plant samples. Plants presenting a common metabolite pattern were used to prevent erroneous interpretations due to atypical behaviour or analytical artefacts.

Metabolite profiling was assessed to confirm the presence of different stress-related compounds. This high-resolution chromatography was found to be essential since a complete deconvolution of the biomarkers was needed for identification purposes and for the resolution of various closely related isomers.

Compared to targeted GC–MS, used in the oxylipin field as a reference technique, the generic characteristics of this two step UPLC–TOF-MS strategy allowed the monitoring in a complex matrix of the wound biomarkers with different physicochemical properties. Since no complex sample preparation is needed, this approach can be used to screen various plant extracts without re-optimisation.

Acknowledgements

Financial support was provided by the Swiss National Science Foundation (Grants no. 205320-107735/1 to J.-L.W. and S.R.). The authors would like to thank Hilary Major for providing the MarkerLynx™ software (Waters, MA, USA).

References

[1] R.D. Hall, New Phytol. 169 (2006) 453.
[2] W.B. Dunn, D.I. Ellis, Trac-Trend Anal. Chem. 24 (2005) 285.
[3] O. Hendrawati, Q. Yao, H.K. Kim, H.J.M. Linthorst, C. Erkelens, A.W.M. Lefeber, Y.H. Choi, R. Verpoorte, Plant Sci. 170 (2006) 1118.
[4] A. Oikawa, Y. Nakamura, T. Ogura, A. Kimura, H. Suzuki, N. Sakurai, Y. Shinbo, D. Shibata, S. Kanaya, D. Ohta, Plant Physiol. 142 (2006) 398.
[5] L.L. Jessome, D.A. Volmer, LC–GC N. Am. (2006) 498.
[6] L. Dubugnon, R. Liechti, E.E. Farmer, 2006, The jasmonate biochemical pathway Connections Map, http://stke.sciencemag.org/cgi/cm/CMP_7361.
[7] E.E. Farmer, E. Almeras, V. Krishnamurthy, Curr. Opin. Plant Biol. 6 (2003) 372.

[8] M.J. Mueller, L. Mène-Saffrané, C. Grun, K. Karg, E.E. Farmer, Plant J. 45 (2006) 472.
[9] O. Fiehn, J. Kopka, P. Dormann, T. Altmann, R.N. Trethewey, L. Willmitzer, Nat. Biotechnol. 18 (2000) 1157.
[10] G. Le Gall, S.B. Metzdorff, J. Pedersen, R.N. Bennett, I.J. Colquhoun, Metabolomics 1 (2005) 181.
[11] K. Cabrera, D. Lubda, H.-M. Eggenweiler, H. Minakuchi, K. Nakanishi, J. High Resol. Chromatogr. 23 (2000) 93.
[12] K. Cabrera, D. Lubda, H.M. Eggenweiler, H. Minakuchi, K. Nakanishi, J. Sep. Sci. 27 (2004) 843.
[13] L. Romanyshyn, P.R. Tiller, J. Chromatogr. A 928 (2001) 41.
[14] L. Romanyshyn, P.R. Tiller, C.E.C.A. Hop, Rapid Commun. Mass Spectrom. 14 (2000) 1662.
[15] D. Guillarme, S. Heinisch, J.L. Rocca, J. Chromatogr. A 1052 (2004) 39.
[16] D. Guillarme, S. Heinisch, Sep. Purif. Rev. 34 (2005) 181.
[17] J.C. Giddings, Anal. Chem. 37 (1965) 60.
[18] J.H. Knox, J. Chromatogr. Sci. 15 (1977).
[19] H. Poppe, J. Chromatogr. A 778 (1997) 3.
[20] R.E. Majors, LC–GC N. Am. 25 (2006) 16.
[21] D.T.T. Nguyen, D. Guillarme, S. Rudaz, J.L. Veuthey, J. Chromatogr. A 1128 (2006) 105.
[22] G. Desmet, D. Clicq, D.T.T. Nguyen, D. Guillarme, S. Rudaz, J.L. Veuthey, N. Vervoort, G. Torok, D. Cabooter, P. Gzil, Anal. Chem. 78 (2006) 2150.
[23] M.E. Swartz, LC–GC N. Am. (2005) 8.
[24] D. Guillarme, D.T.T. Nguyen, S. Rudaz, J.L. Veuthey, J. Sep. Sci. 29 (2006) 1836.
[25] I.S. Lurie, J. Chromatogr. A 1100 (2005) 168.
[26] S.A.C. Wren, P. Tchelitcheff, J. Chromatogr. A 1119 (2006) 140.
[27] J.R. Mazzeo, U.D. Neue, M. Kele, R.S. Plumb, Anal. Chem. 77 (2005) 460A.
[28] I.D. Wilson, J.K. Nicholson, J. Castro-Perez, J.H. Granger, K.A. Johnson, B.W. Smith, R.S. Plumb, J. Proteome Res. 4 (2005) 591.
[29] R.S. Plumb, J.H. Granger, C.L. Stumpf, K.A. Johnson, B.W. Smith, S. Gaulitz, I.D. Wilson, J. Castro-Perez, Analyst 130 (2005) 844.
[30] A. Nordstrom, G. O'Maille, C. Qin, G. Siuzdak, Anal. Chem. 78 (2006) 3289.
[31] E.C.Y. Chan, S.L. Yap, A.J. Lau, P.C. Leow, D.F. Toh, H.L. Koh, Rapid Commun. Mass Spectrom. 21 (2007) 519.
[32] E. Grata, J. Boccard, G. Glauser, P.A. Carrupt, E.E. Farmer, J.L. Wolfender, S. Rudaz, J. Sep. Sci. 30 (2007) 2268.
[33] D.C. Boyes, A.M. Zayed, R. Ascenzi, A.J. McCaskill, N.E. Hoffman, K.R. Davis, J. Görlach, Plant Cell 13 (2001) 1499.
[34] G. Desmet, D. Clicq, P. Gzil, Anal. Chem. 77 (2005) 4058.
[35] J. Boccard, E. Grata, A. Thiocone, J.Y. Gauvrit, P. Lanteri, P.A. Carrupt, J.L. Wolfender, S. Rudaz, Chemometr. Intell. Lab. Syst. 86 (2007) 189.
[36] Kinetic plot analyzer download, http://wwwtw.vub.ac.be/CHIS//research/tmas2/kineticplot/kineticplot.html.
[37] A. Maruska, O. Kornysova, J. Chromatogr. A 1112 (2006) 319.
[38] V.V. Tolstikov, A. Lommen, K. Nakanishi, N. Tanaka, O. Fiehn, Anal. Chem. 75 (2003) 6737.
[39] V.V. Tolstikov, O. Fiehn, N. Tanaka, Methods Mol. Biol. 358 (2007) 141.
[40] D. Guillarme, D.T.T. Nguyen, S. Rudaz, J.-L. Veuthey, Eur. J. Pharm. Biopharm. 68 (2008) 430.
[41] C. Wasternack, I. Stenzel, B. Hause, G. Hause, C. Kutter, H. Maucher, J. Neumerkel, I. Feussner, O. Miersch, J. Plant Physiol. 163 (2006) 297.
[42] L. Li, C.Y. Li, G.I. Lee, G.A. Howe, Proc. Natl. Acad. Sci. U.S.A. 99 (2002) 6416.
[43] C. Li, A.L. Schilmiller, G. Liu, G.I. Lee, S. Jayanty, C. Sageman, J. Vrebalov, J.J. Giovannoni, K. Yagi, Y. Kobayashi, G.A. Howe, Plant Cell 17 (2005) 971.
[44] P. Reymond, H. Weber, M. Damond, E.E. Farmer, Plant Cell 12 (2000) 707.
[45] J.W. Dolan, L.R. Snyder, J. Chromatogr. A 799 (1998) 21.
[46] A.P. Schellinger, P.W. Carr, J. Chromatogr. A 1077 (2005) 110.
[47] Laboratory of analytical pharmaceutical chemistry (LCAP), HPLC calculator download, In: LCAP website (on-line), http://www.unige.ch/sciences/pharm/fanal/lcap/index.htm.
[48] H. Weber, B.A. Vick, E.E. Farmer, Proc. Natl. Acad. Sci. U.S.A. 94 (1997) 10473.
[49] P.E. Staswick, I. Tiryaki, Plant Cell 16 (2004) 2117.
[50] G. Glauser, D. Guillarme, E. Grata, J. Boccard, A. Thiocone, P.-A. Carrupt, J.-L. Veuthey, S. Rudaz, J.-L. Wolfender, J. Chromatogr. A 1180 (2008) 90.